JOURNAL OF THE ROYAL SOCIETY Interface

rsif.royalsocietypublishing.org

Research

Cite this article: Lehmann F-O, Skandalis DA, Berthé R. 2013 Calcium signalling indicates bilateral power balancing in the *Drosophila* flight muscle during manoeuvring flight. J R Soc Interface 10: 20121050.
http://dx.doi.org/10.1098/rsif.2012.1050

Received: 21 December 2012
Accepted: 22 February 2013

Subject Areas:
biomechanics

Keywords:
flight energetics, muscle mechanical power, calcium imaging, cameleon, FRET, *Drosophila*

Author for correspondence:
Fritz-Olaf Lehmann
email: fritz.lehmann@uni-rostock.de

Electronic supplementary material is available at http://dx.doi.org/10.1098/rsif.2012.1050 or via http://rsif.royalsocietypublishing.org.

Royal Society Publishing
Informing the science of the future

Calcium signalling indicates bilateral power balancing in the *Drosophila* flight muscle during manoeuvring flight

Fritz-Olaf Lehmann, Dimitri A. Skandalis and Ruben Berthé

Department of Animal Physiology, University of Rostock, Albert-Einstein-Strasse 3, Rostock 18059, Germany

Manoeuvring flight in animals requires precise adjustments of mechanical power output produced by the flight musculature. In many insects such as fruit flies, power generation is most likely varied by altering stretch-activated tension, that is set by sarcoplasmic calcium levels. The muscles reside in a thoracic shell that simultaneously drives both wings during wing flapping. Using a genetically expressed muscle calcium indicator, we here demonstrate *in vivo* the ability of this animal to bilaterally adjust its calcium activation to the mechanical power output required to sustain aerodynamic costs during flight. Motoneuron-specific comparisons of calcium activation during lift modulation and yaw turning behaviour suggest slightly higher calcium activation for dorso-longitudinal than for dorsoventral muscle fibres, which corroborates the elevated need for muscle mechanical power during the wings' downstroke. During turning flight, calcium activation explains only up to 54 per cent of the required changes in mechanical power, suggesting substantial power transmission between both sides of the thoracic shell. The bilateral control of muscle calcium runs counter to the hypothesis that the thorax of flies acts as a single, equally proportional source for mechanical power production for both flapping wings. Collectively, power balancing highlights the precision with which insects adjust their flight motor to changing energetic requirements during aerial steering. This potentially enhances flight efficiency and is thus of interest for the development of technical vehicles that employ bioinspired strategies of power delivery to flapping wings.

1. Introduction

The evolutionary success of flying insects is due in large part to their ability to produce and control aerodynamic forces during wing flapping. To allow fine control of wing flapping from stroke-to-stroke while producing elevated muscle power, insects such as the tiny fruit fly *Drosophila* use two different muscle systems: synchronously activated flight control muscles and asynchronous, indirect flight muscles (A-IFMs) that deliver the power for wing flapping [1–6]. The A-IFM causes wing motion by an indirect linkage between muscle and wings and benefits from the elastic and resonance properties of the thorax shell [7]. During steering, flight control muscles reconfigure the wing hinge of the thoracic oscillator, controlling mechanical properties of the thorax and thus power transmission from the A-IFM to the flapping wings [8–14].

The elevated power requirements for wing flapping in dipterans results from high aerodynamic drag associated with lift production at relatively low Reynolds numbers (*Drosophila*, $Re = 134$, [15]), produced at exceptionally high wing flapping frequencies of up to 1000 Hz [16]. Asynchronous power muscles cope with these requirements by avoiding energetic expenditures of stroke-to-stroke calcium pumping and thus rapid changes in intramuscular calcium, at the cost of power control [17]. In contrast to the contraction cycle of the synchronous striated muscle, asynchronous muscle twitching is thus synchronized with wing flapping frequency rather than muscle spike frequency [18]. In tethered flying *Drosophila*, wing flapping frequency is approximately 40 times higher than muscle spike frequency, amounting to approximately 200 and 5 Hz at room temperature, respectively [19]. Therefore, for many years the A-IFM's

neural input was considered to be a simple trigger for myoplasmic calcium levels above a critical threshold, switching the flight motor on and off in order to start and terminate wing motion, respectively [18,20,21].

Other studies, moreover, suggested that the A-IFM's low spike frequency maintains rather constant calcium levels during flight [22]. Calcium-activated muscle tension, however, is comparatively small in *Drosophila* A-IFM, producing only approximately 30 per cent of total tetanic contraction by actin–myosin cross-bridge cycling [23,24]. Similar low tension has been reported for muscles of the giant water bug *Lethocerus* at physiological ion strength [25]. As the calcium-activated isometric force component may not account for all power required to sustain active flight, stretch activation owing to 1.0–2.5% alterations in fibre length increases the number of cross-bridge cycles of the calcium-activated muscle [23]. This cross-bridge recruitment leads to a delayed threefold to fourfold increase in force during muscle shortening and hence increased muscle work and power generation within each stroke cycle [17,26]. Shortening deactivation decreases force levels during lengthening by decreasing the number of cross-bridges, which attenuates muscle stiffness when the fibres undergo their cyclic shortening–lengthening cycle [5,27–32]. In general, the function of the A-IFM in *Drosophila* is similar to the vertebrate cardiac muscle, to generate power during oscillatory contractions and thus beneficial for understanding muscle function in a larger context. This includes, for example, studies on the functional significance of structural alterations of muscle myosin for muscle tension and power [33–37], the muscle proteins obscurin [38], troponin [39] and fligthin [40], ageing effects such as age-dependent degradation of muscle ultrastructure and mitochondrial damage [41], and muscle mechanical properties of the A-IFM [26].

The above calcium-switching hypothesis was recently questioned by two studies on calcium-mediated power control of *Drosophila*'s A-IFM fibres, demonstrating that increasing $[Ca^{2+}]$ inside the A-IFM leads to increasing power output during cyclic stretching in skinned fibres using work-loop technique [24] and in tethered flying flies [19]. The first study showed a steep increase in positive muscle power with increasing pCa within a small range of calcium from pCa = 5.0 to pCa = 5.8, whereas the second *in vivo* study suggested a twofold increase of $[Ca^{2+}]$ within the working range of the thoracic flight motor. The *in vivo* study did not score, however, how calcium signalling is spatially distributed between various fibres of the A-IFM during flight manoeuvres of *Drosophila*, especially when power requirements for wing flapping are not balanced between both body sides. Thus, it remained unclear of how muscle power, which is the sum of calcium- and stretch-activated power, alters between the left and right dorso-longitudinal muscle (DLM) and dorsoventral muscle (DVM) fibres of the A-IFM during lift and turning manoeuvres. In particular, turning flight requires an asymmetrical distribution of flight muscle power owing to asymmetrical drag production on both wings. A flight system that supports these asymmetries on the level of neural control might thus be beneficial for power balancing.

To demonstrate how *Drosophila* controls intramuscular calcium levels in each of the 24 A-IFM fibres during various flight behaviours to achieve bilateral balance in muscle power and to satisfy asymmetrical power requirements for flapping flight, we simultaneously determined mechanical power required for wing flapping and calcium activation during tethered flight of transgene fruit flies, genetically expressing the calcium indicator cameleon. While continuously measuring stroke frequency and amplitude of both wings, we elicited flight manoeuvres by visual stimulation of the fly's compound eye, making use of the animal's optomotor reflexes [42,43]. We further demonstrate that mechanical power increases with increasing calcium within a comparatively small range of intramuscular $[Ca^{2+}]$, matching previously published results, and suggest that the cuticular shell of the thorax redirects muscle mechanical power between left and right body side during turning flight.

2. Experimental details

2.1. Mechanical power estimation

Owing to the difficulties in determining the mechanical power output of flight muscles *in vivo*, many biomechanics estimate mechanical power from power requirements for wing flapping rather than from direct force measurements. This concept is widely spread and especially used in small animals such as insects [19,44–47]. Estimates of power requirements result from biomechanical and aerodynamic considerations such as energetic cost to overcome wing inertia (inertial power) during flapping motion, aerodynamic drag on wings (profile power), the energetic costs to generate lift (induced power) and drag on the animal body during forward motion (parasite power). The contribution of each of these components to total power varies depending on flight manoeuvres and aerodynamic assumptions [12]. Assuming 100 per cent elastic energy storage of the wing's kinetic energy inside the thorax during wing flapping, A-IFM mechanical power output of a tethered flying *Drosophila* equals the sum of induced and profile power requirements [7].

We estimated induced and profile muscle mass-specific flight power requirements from wing velocity, several fly-specific morphological parameters of the wing and stroke-wise lift and drag production. Wing velocity was determined from the product of stroke frequency and amplitude, measured via a piezo transducer attached to the fly's body and from the ventral and dorsal wing excursion recorded on infrared video images, respectively (figure 1*a*). As our experimental approach did not allow simultaneous force measurements, instantaneous lift and drag were estimated from their corresponding force coefficients. According to the data published previously for *Drosophila* flying attached to a force balance, we used a mean lift coefficient of 1.59 for wing flapping while—owing to the difficulty in measuring profile drag in flying animals—the mean drag coefficient of 0.94 was estimated from polars determined under three-dimensional flapping conditions in a dynamically scaled robotic *Drosophila* model wing [15,40,49]. The latter approach considers all major drag enhancing unsteady aerodynamic mechanisms present in *Drosophila* flight and provides a comparatively precise force estimate based on stroke frequency and amplitude measurements. All equations used for energetic modelling are outlined in the electronic supplementary material. In contrast to previous studies, however, muscle mechanical power output was determined separately for each body side, according to wing motion and flight force derived from aerodynamic theory [7,12]. The entire procedure allowed us to obtain an *in vivo* measure for left–right muscle mechanical power

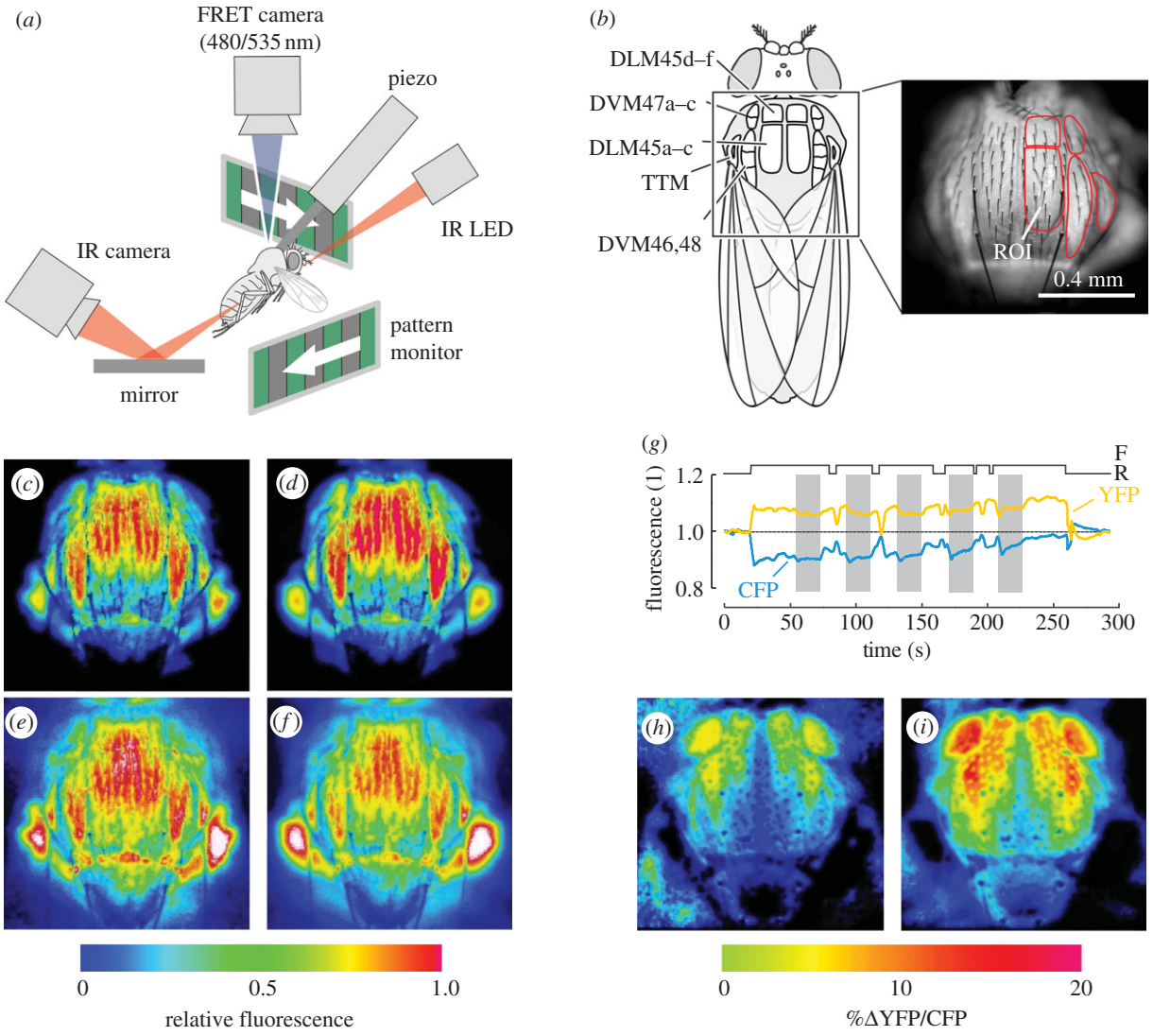

Figure 1. Methods and FRET imaging. (*a*) Experimental setup for in-flight calcium imaging of the indirect flight muscle (A-IFM) of transgene *Drosophila* cameleon 2.1. The fly is tethered to a piezo transducer to monitor stroke frequency, and left and right stroke amplitudes are measured from infrared video images of the flapping wings, illuminated by an infrared light emitting diode (IR LED). The fly is visually stimulated by the motion of two stripe patterns. A fluorescence imaging microscope with 440 nm excitation wavelength records emission wavelengths of 480 and 535 nm while the animal responds to the visual stimulation. (*b*) Nomenclature for A-IFM adopted from Demerec [48]. Left, muscle attachment sites of the flight muscle on the inner cuticle of the thorax (dorsal view). Right, example of regions-of-interest (ROI) to determine FRET in individual muscle fibres, superimposed with YFP fluorescence image. (*c–f*) Fluorescence images of YFP (535 nm; *c,d*) and CFP (480 nm; *e,f*) during rest (left) and flight (right) plotted in pseudo-colour. For thorax orientation refer to (*b*). (*g*) Changes in YFP and CFP fluorescence during flight and rest, and during visual stimulation (grey, optomotor yaw). (*h*) Relative YFP/CFP ratio (FRET) in a resting and (*i*) in a flying fly. Data are plotted in pseudo-colour and normalized to mean YFP/CFP ratio during rest. Flight-mediated increase in YFP/CFP ratio is similar to the increase caused by electrical stimulation of the A-IFM (see the electronic supplementary material, figure S3). Images are taken from a 93 s video sequence (see the electronic supplementary material, movie S1). DVM, dorsoventral muscle; DLM, dorso-longitudinal muscle; F, time of flight; R, time of rest; YFP, yellow fluorescence protein; CFP, cyan fluorescence protein.

balance based on the power required for flapping each of the two wings, without interfering with the thorax's mechanical system during wing flapping.

2.2. Experimental procedure and visual stimulation

The tested animals were flown in an experimental setup in which A-IFM calcium activation and muscle mechanical power output were simultaneously and continuously measured (figure 1*a*). In total, we analysed behavioural sequences from 25 transgene, 5–7 day old females with a mean body mass of 1.06 $\pm$ 0.13 mg. Each sequence was 293 s and consisted of two 30 s resting periods at the beginning and the end, and a 235 s flight sequence, in which flight power was modulated by visual stimulation of the fly's compound eyes [12]. We achieved this by employing two 30 mm high and 50 mm wide small optic screens that displayed horizontally moving green–black visual stripe patterns with 26° spatial wavelength and 2.2 Hz visual contrast frequency. The two screens were placed laterally of the two eyes (figure 1*a*). The pattern motions induced either optomotor yaw manoeuvres (asymmetrical pattern motion) or lift/thrust responses (symmetrical pattern motion) and changed direction every 20 s. Pattern motion direction and angular velocity were controlled by a self-written software program and temporally synchronized with image capture of wing motion and calcium signalling.

2.3. Generation of transgenic flies and calcium measurements

To examine the relationship between muscle mechanical power output and calcium activation in flight, we genetically

expressed the intramuscular, fluorescent Ca^{2+} reporter cameleon 2.1 (Cam2.1) in *Drosophila melanogaster* [50–53]. The Cam2.1 indicator signals calcium by two fluorescence domains (yellow fluorescent protein, YFP and cyan fluorescent protein, CFP) owing to calcium-dependent fluorescence resonance energy transfer (FRET; [54,55]). FRET allows estimations of intramuscular calcium levels independent of changes in total A-IFM fluorescence. The two fluorescence proteins were activated with light at 440 nm, which was precisely focused on the dorsal, intact thorax of the fly, whereas light emission of the proteins occurred at 480 nm (CFP) and 535 nm (YFP), respectively (figure 1*c–g*). Following previous approaches, the change in calcium concentration (%ΔYFP/CFP) was subsequently derived from the difference in FRET signal strength from rest to flight, normalized to FRET at rest [19] (figure 1*h,i*). For more detailed information see supplemental material.

For calcium imaging, we used a dual emission fluorescence microscope for two-channel-FRET (Axioscope 2 FS plus, Zeiss). An optical beam splitter separated the two emission wavelengths, so that both images were simultaneously recorded by a peltier-cooled video camera (AxioCam MRm, Zeiss). We scored FRET signals for each of the A-IFM fibres inside the fly's thorax by tracing the perimeter of the thoracic muscle attachment sites on the video image (region-of-interests, ROIs) and subsequently averaging all video pixels within each ROI (figure 1*b*). Size and shape of each ROI were individually adjusted for each fly according to body size and orientation. During manoeuvring flight, we simultaneously recorded time-resolved FRET changes at 6.48 Hz sampling frequency in eight DLM and DVM fibres, including the synchronously activated tergo-trochanter 'jump' muscle of the middle leg for comparison, each identified from their cuticular attachment sites on the inner side of the dorsal thorax [56]. A detailed comparison of calcium balancing between single muscle fibres eventually allowed us to determine fibre-specific calcium activation gains within the thoracic flight motor.

3. Results and discussion

On flight initiation of *Drosophila*, mean calcium signalling (FRET) of left and right DVM and DLM fibres increases transiently by approximately 30 per cent, and eventually saturates at approximately 12 per cent compared with rest (rest: 4.46 ± 0.14 YFP/CFP, flight: 5.07 ± 0.19 YFP/CFP, means ± s.d., $n = 102$ flight sequences, figures 1*h,i* and 2). Although the synchronously activated tergo-trochanter muscle (TTM) of the middle legs shows similar dynamics as A-IFM, its FRET activation increases by only 26.9%ΔFRET W^{-1} g with increasing A-IFM power output (figure 3*b* and table 1), which is significantly different from all A-IFM subsets (*t*-test on slope, $p < 0.001$ for all fibres; electronic supplementary material, table S2). It is probably that TTM activation reflects optical crosstalk between muscle fibres or occasional leg movements, because the middle legs are typically not involved in steering control during flight of flies but during landing response [58]. Optomotor visual stimulation of the flying animal produces significant alterations in FRET of all measured A-IFM fibres. We monitored these changes to identify spatio-temporal trends in calcium signalling with A-IFM power output.

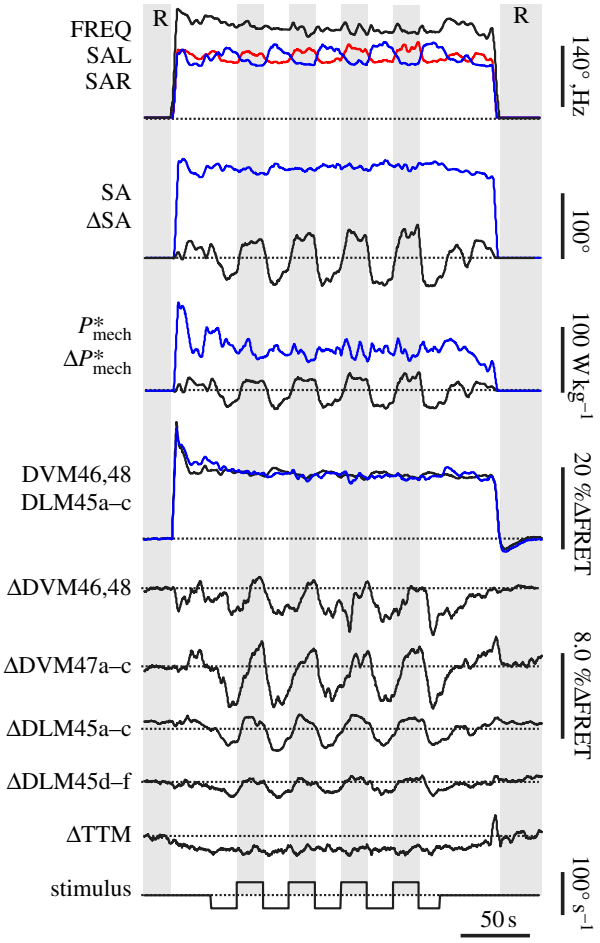

Figure 2. Wing kinematics and FRET of *Drosophila* A-IFM at rest (R) and in flight during optomotor yaw response. Traces show left stroke amplitude (SAL, red), right stroke amplitude (SAR, blue), stroke frequency (FREQ, black), mean stroke amplitude of both wings (SA, blue), left-minus-right stroke amplitude difference (ΔSA, black), the corresponding outputs of total mass-specific A-IFM mechanical power (P^*_{mech}, blue) and power difference (ΔP^*_{mech}, black) and the changes in mean FRET of A-IFM fibres, scored from thoracic muscle attachment sites for left and right dorsoventral muscle (DVM46,48, black) and dorso-longitudinal muscle (DLM45a–c, blue). The traces below show left-minus-right difference (Δ) in FRET of selected A-IFM fibres and the calcium activation of the synchronous tergo-trochanter muscle (TTM) of the animal's middle leg. Stimulus velocity of the visual pattern is shown at the bottom, where positive (negative) values indicate optomotor yaw stimulation to the right (left). The traces are typical of the measured animals and were simultaneously recorded in a single fly. Zero is indicated by a dotted line.

3.1. Lift and thrust modulation

In response to bilaterally directional changes of the moving stripe patterns (lift/thrust modulation), A-IFM mass-specific mechanical power changes over an approximately eightfold range, from 20 to 160 W kg^{-1} flight muscle mass (figures 2 and 3*b*). However, owing to calcium saturation at a power production above 120 W kg^{-1}, we generally limited our statistical regression analysis to data ranging from 20 to 120 W kg^{-1} muscle mass. Maximum calcium signalling above 120 W kg^{-1} ranges from 17.0%ΔFRET in fibres of the DLM45d–f and DVM47a–c to 19.2%ΔFRET in DVM46,48 fibres (table 1). Saturation of FRET was not noted during electrical stimulation of A-IFM via the fly's giant fibre pathways with stimulus frequencies of up to 25 Hz, which is threefold the maximum A-IFM spiking frequency measured during tethered flight in *Drosophila* [19]. Moreover, our FRET signals

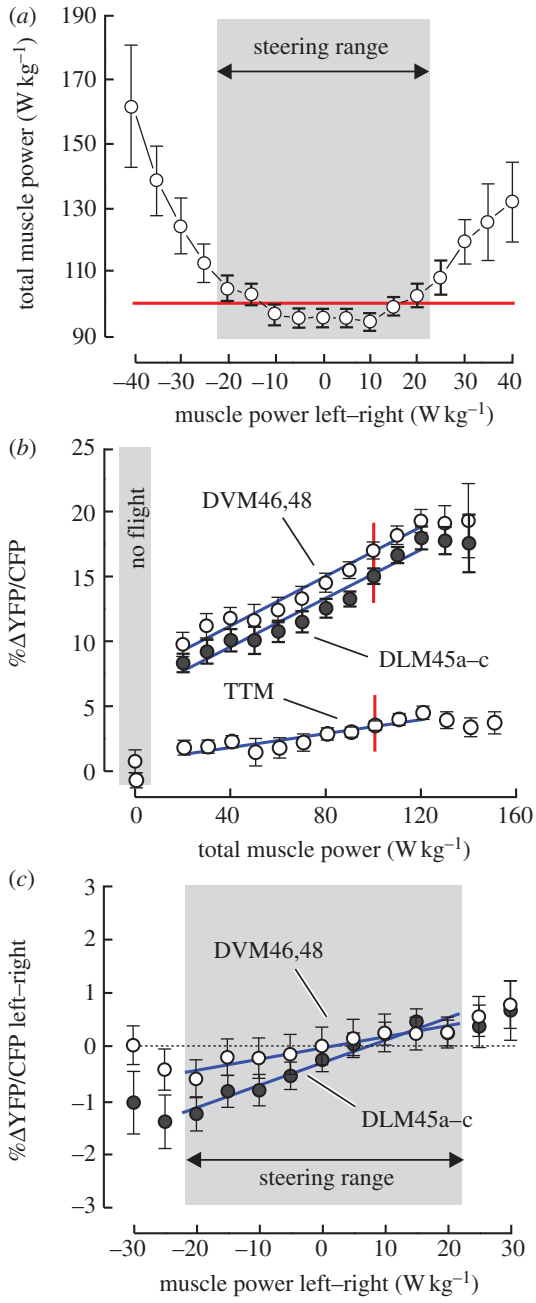

Figure 3. Changes in IFM calcium activation with changing muscle mass-specific mechanical power output during flight. (*a*) Total A-IFM power requirements during yaw turning behaviour, during which left–right power requirements typically vary between ± 20 W kg^{-1} flight muscle mass. (*b*) Relative increase of mean (left, right body side) calcium concentration in DVM46,48 fibres and DLM45a–c fibres owing to FRET. Grey area indicates values at rest. Data are binned with a bin size of 10 W muscle mechanical power output per kg A-IFM mass. Number of flight sequences of each mean value from left to right is 7, 12, 18, 23, 24, 25, 25, 25, 22, 22, 20, 18, 11 and 5. (*c*) Calcium activation in DVM and DLM fibres during optomotor yaw manoeuvres in which the fly increases its stroke amplitude on one side while decreasing it on the other. Difference in YFP/CFP ratio between left and right body side is plotted against asymmetrical changes in muscle mechanical power output (left-minus-right, $n = 21$ flies). Data are typical of all A-IFM fibres. Grey area indicates typical range of optomotor-induced alteration of mechanical power. Muscle mechanical power that supports the fly's body weight is indicated by the red line in (*a*). Blue, linear regression fit. For visual clarity, means are presented $\pm$ s.e.

varied by at most 35 per cent and were thus always within the 1.6-fold dynamic range reported for Cam2.1 *in vivo* measurement [52,53]. Thus, it is less probably that FRET

Table 1. Calcium activation slopes and fibre-specific comparison of asynchronous indirect flight muscle (A-IFM) during flight of transgene Cam2.1 *Drosophila*. Slopes are calculated from linear regressions to binned mean FRET values and A-IFM mass-specific power estimates. Note that DLM45a–c employs only two motor neurons for three muscle fibres [57]. Data were recorded from flight sequences of 25 flies, where each sequence was approximately 5 min. Maximum mean %ΔFRET saturates between 120 and 140 W kg^{-1} muscle (mean $\pm$ s.d.). *R*, correlation coefficient; *p*, probability; n.a., not applicable; TTM, tergo-trochanter musde.

muscle	fibres	%ΔFRET maximum	%ΔFRET W^{-1} g^{a}	R^{2a}	p^{a}_{slope}	%ΔFRET W^{-1} g^{a,b}	%ΔFRET W^{-1} g^{c}	R^{2c}	p^{c}_{slope}	yaw/lift slope ratio (%)	p^{d}_{slope}
DLM45a–c	2	17.9 $\pm$ 1.39	91.7	0.95	<0.001	45.9	28.1	0.94	<0.001	30.6	<0.001
DLM45d–f	3	17.0 $\pm$ 1.14	85.3	0.95	<0.001	28.4	14.6	0.80	<0.002	17.1	0.001
DVM46,48	4	19.2 $\pm$ 1.70	91.7	0.96	<0.001	22.9	20.1	0.89	<0.001	21.9	<0.001
DVM47a–c	3	17.0 $\pm$ 1.51	81.3	0.97	<0.001	27.1	44.0	0.88	<0.001	54.1	0.004
TTM	n.a.	4.09 $\pm$ 0.62	26.9	0.81	<0.001	n.a.	−5.8	0.66	0.008	−21.6	0.003

[a]Linear regression slope during optomotor lift stimulation at flight power ranging from 20 to 120 W kg^{-1} muscle mass.
[b]Motor neuron-specific value.
[c]Regression slope during yaw stimulation for power ranging from −20 to 20 W kg^{-1} muscle mass.
[d]*t*-test on slope difference between lift and yaw stimulation.

saturation in figure 3*b* results from a limit in the cameleon's calmodulin binding capacity to intramuscular calcium within the physiological range of A-IFM spike frequency.

By contrast, saturation was previously measured in an *in vitro* study on *Drosophila* A-IFM using work-loop analysis [24]. The data show that dissected A-IFM fibres start to produce positive power at pCa = 5.0, power increases with increasing calcium and saturates at approximately 400 W m^{-3} muscle volume above pCa = 5.8. Notably, the latter finding runs counter to our finding that calcium activation saturates while power increases and not vice versa. The *in vitro* result thus supports the idea of limited cross-bridge cycling activation at muscular pCa above 5.8, in turn limiting power output and thus flight force production [24]. The *in vivo* saturation shown in figure 3*b*, by contrast, suggests power augmentation above 120 W kg^{-1} without increasing calcium. A potential explanation of this finding is strain-dependent power augmentation during cyclic stretch activation of A-IFM fibres. During flight, *Drosophila* increases power output by increasing both muscle spiking frequency and stroke amplitude of the wing [11,19]. Stroke frequency increases with increasing power only at flight forces below hovering force but saturates at elevated forces at approximately 212 Hz [12]. It has further been suggested that owing to the mechanical design of the thorax, in-flight thorax deformation probably increases with increasing stroke amplitude because thorax strain amplitude may vary within individual cycles from 2 to 5 per cent of the A-IFM resting length [59]. In turn, thorax deformation causes appropriate changes in A-IFM fibres length. As stretch-activation muscle tension has been shown to vary with myoplasmic [Ca^{2+}] in fibres of *Lethocerus* A-IFM, an increase in thorax deformation should result in an increase in stretch-activated muscle tension [60–62]. In *Drosophila*, however, the maximum sum of *in vitro* muscle tension (calcium-plus stretch-activated tension) shows only minor differences between stretch activation at 1.0 and 2.5 per cent length change, but larger lengthening steps produce higher stretch-activated tension in both the deactivated (pCa = 8.0; 5.5 and 11.4 mN mm^{-2}, respectively) and fully activated muscle (pCa = 4.5; 1.5 and 11 mN mm^{-2}, respectively, [24]). Despite the small difference in total force, we thus suggest that stretch-dependent power augmentation in intact A-IFM fibres of *Drosophila* might enhance total power output considering the controversial debate on the interplay between calcium- and stretch-activated tension of *Lethocerus* IFM [60–62].

Within the 20–120 W kg^{-1} range, the fluorescent signal of all A-IFM fibres approximately doubles, increasing with minimum slopes of 81.3 in DVM47a–c fibres and maximum slopes of 91.7%ΔFRET W^{-1} g total flight muscle mass in fibres of the DLM45a–c and DVM46,48 (table 1). A similar twofold increase of [Ca^{2+}] inside the A-IFM was also found by Gordon & Dickinson [19] during tethered *Drosophila* flight, when calcium was solely correlated with the changes in aerodynamic power and A-IFM motor nerve firing frequency. The high mean correlation coefficient squared of approximately 0.96 during lift stimulation suggests that changes in A-IFM mechanical power output are fully supported by equivalent changes in FRET in all fibres, and thus by equivalent neural activation (table 1). This finding is consistent with the lack of motor recruitment, i.e. the number of active fibres to increase mechanical power [63] in small insects [24]. While the sum of left and right A-IFM power and calcium activation increases with flight force production, the left-minus-right differences of mechanical power ($y = 1.87 + 0.01x$ W kg^{-1}, $p = 0.23$) and calcium activation of all fibres ($y = 9.70 + 2.11x$ %ΔFRET W^{-1} g muscle mass, $p = 0.19$) change comparatively little, indicating bilateral equal changes in both wing motion and neural activation during lift response. Consequently, in a freely manoeuvring fly, the latter finding would cause changes in flight altitude without distinctive changes in horizontal flight heading.

For estimation of calcium activation at hovering flight conditions, we calculated aerodynamic lift production from wing stroke amplitude and stroke frequency as outlined in the electronic supplementary material. Hovering flight in *Drosophila* is energetically demanding because all lift is produced by the animal's own wing motion [46]. Hovering flight conditions have thus previously been used for interspecific comparison in fly flight [49]. Our data show that the fruit fly compensates its body weight at an A-IFM power output of approximately 100 W kg^{-1} muscle mass (figure 3*a*), while flapping the wings at mean amplitude and frequency of 152 ± 2.27° and 227 ± 2.40 Hz, respectively (means ± s.d., $n = 25$ flies). For comparison, a previous study reported stroke amplitudes ranging from 130° to 155° and mean frequencies near 200 Hz, while the tethered fruit fly altered A-IFM mechanical power production between approximately 50 and 80 W kg^{-1} muscle mass [19]. At hovering flight conditions, A-IFM calcium activation is scattered around 15.4 ± 1.18%ΔFRET, which corresponds to approximately 87 per cent of the maximum calcium activation (mean ± s.d., $n = 4$ muscle fibres; figure 3*b* and table 1). The small 13 per cent difference between hovering and maximum calcium activation might be of significance with respect to the potential role of calcium activation for the fly's maximum lift capacity, i.e. 1.6 times body weight [49]. We hypothesize that the small range of calcium activation capacity at flight forces above body weight might constrain muscle power at peak flight performance, which compares with performance limits set by the oxygen supply capacity of the insect's tracheal system [64–66].

3.2. Muscle fibre-specific activation

Calcium activation is A-IFM fibre-specific during flight. All A-IFM subsets yield different mean FRET with increasing A-IFM power output (paired *t*-test, $p < 0.05$): mean FRET of the DLM46,48 fibres is 1.64 and 2.15%ΔFRET higher than in fibres of DLM45a–c and DLM45d–f, respectively, DLM45a–c–f is 0.36%ΔFRET higher than DVM47a–c, and DLM 45d–f is 0.86%ΔFRET higher than in fibres of the DVM47a–c. However, these differences are relatively small and may only account for negligibly small changes in muscle mechanical power output. The same holds for the calcium activation slopes during aerodynamic lift modulation because all A-IFM regression coefficients are significantly similar ($p > 0.05$, $n = 4$ fibres; electronic supplementary material, table S2). Nevertheless, the fibres of the DLM receive a stronger neural drive (28.4–45.9%ΔFRET W^{-1} g) than those of the DVM (22.9–27.1%ΔFRET W^{-1} g total muscle mass) when normalized to the number of driving motor neurons associated with this muscle subset (table 1). We found significant slope differences (*t*-test on slope) between fibres of the DVM47a–c and DLMa–c ($p < 0.001$), DVM46,48 and DLM45a–c ($p < 0.001$), DVM46,48 and DLM45d–f ($p < 0.05$), and DLM45a–c and DLM45d–f ($p < 0.001$). Other fibre comparisons were not significantly different ($p > 0.05$).

With respect to aerodynamic power expenditures, the latter results might match the temporal distribution of power requirements within the stroke cycle of *Drosophila*. Force analyses using robotic *Drosophila* wings demonstrated approximately 1.8 times more drag on the flapping wings during the downstroke than the upstroke (0.44 versus 0.25 N), which converts into 42 per cent higher aerodynamic power requirements for wing flapping during the downstroke [15,67]. We derived similar results from a numerical study on aerodynamic forces using *Drosophila* free flight kinematics [68]. The higher motor neuron-specific calcium activation slope of muscle fibres driving the fruit fly wing downward, which are the fibres of the DLM, might thus be a beneficial adaptation of the flight apparatus to cope with the changes in aerodynamic power requirements during wing flapping. Moreover, as the higher regression slope for DLM indicates a lower calcium activation gain (slope inverse), the neural drive to the DLM might control mechanical power output more precisely than the neural circuitry controlling DVM function. Thus, given the limits of A-IFM spike frequency control in flies, the calcium-dependent power adjustments during the wings' downstrokes might better match the exact power requirements for flight compared with the upstroke.

3.3. Calcium signalling during optomotor yaw stimulation

In contrast to the equal changes in wing motion during optomotor lift stimulation, optomotor yaw stimulation, in which the two stripe patterns move into opposite directions, induces changes in relative stroke amplitude between left and right body sides. Under these conditions, mean stroke amplitude and stroke frequency change comparatively little (figure 2). Relative changes in stroke amplitude within the typical steering range lead to asymmetrical changes in flight power requirements for the two flapping wings, and thus to changes in the balance of muscle mechanical power output between both body sides of approximately $\pm 20\ \mathrm{W\ kg^{-1}}$ A-IFM mass (grey area, figure 3*a*,*c*). By contrast, reinforced yaw turning outside the typical $\pm 20\ \mathrm{W\ kg^{-1}}$ range for steering leads to a pronounced increase in total power requirements of both wings (figure 3*a*). We attribute this finding to the following mechanism: the curved flight path during free flight yaw turning is an accelerated trajectory at which the acceleration requires the action of a centripetal force acting against centrifugal force. The centripetal force keeps the animal on the curved track and avoids side slipping. A force balance model on *Drosophila* free flight has demonstrated that centripetal forces may account for up to 70 per cent of total force production in this animal, whereas wing drag-induced yaw moments around the vertical body axis require forces of only 3–5% total flight force [69]. Although the animal was tethered in the present study, the flight apparatus underlying the neural control system nearly doubled the total power output of both wings at the maximum yaw steering response (figure 3*a*). We propose that this neuronal activation pattern is a pre-adaption in anticipation of a turn and thus part of an inherent flight control strategy in flies, helping the animals to adjust A-IFM power output to their power requirements during manoeuvring flight.

Despite the common mechanical drive of both wings by the thoracic exoskeleton, the asymmetries in power requirements for wing flapping are corroborated by accompanying changes in A-IFM FRET signalling. In accordance with the direction of steering, FRET difference between left and right muscle fibres increases with increasing relative stroke amplitude with a mean slope of approximately $26.7\%\Delta\mathrm{FRET\ W^{-1}\ g}$ flight muscle mass (mean $R^2 = 0.88$; figure 3*c* and table 1), whereas %ΔFRET averaged over both body sides does not change under this flight condition (*t*-test on regression coefficient, $p > 0.05$ in all fibres). The asymmetrical activation of left and right A-IFM runs counter to the conventional view on the dipteran flight motor, suggesting a strict division of labour between A-IFM power delivery and wing control by steering muscles [70]. Instead, our findings suggest that turning control in *Drosophila* is not exclusively owing to the activity and function of the tiny synchronous flight control muscles but is also supported by bilateral changes in calcium balancing in the asynchronous flight power muscles.

3.4. Bilateral power transmission

Although the indirect flight musculature is bilaterally controlled during yaw manoeuvres, the calcium activation slope of A-IFM is 1.9–5.8 times lower during optomotor yaw stimulation than during lift stimulation. This finding suggests that during directional turning at which left and right body sides require different amounts of power for wing flapping, the nervous system unilaterally controls A-IFM power output by calcium activation, but its neural drive balances calcium only to 17–54% of the value expected from calcium activation during aerodynamic lift control (table 1).

The other way round: 46–83% of the changes in unilateral power requirements during turning are not supported by unilateral A-IFM calcium activation. More than two-third of the bilateral power difference is thus probably due to power transmission between left and right body sides through the thoracic exoskeleton of the animal (figure 1*b*). Consequently, the unilateral neural control of A-IFM calcium during turning flight might be regarded as a mechanism that finely supports power balancing by bilateral thoracic power shifting, potentially allowing a higher precision in control of actin–myosin cross-bridge cycling. In sum, our results suggest an extended, complex model for unilateral control of aerodynamic forces in *Drosophila* that includes not only neural activity within the 18 flight control muscles of the fly [2], but also fibre-specific neural control of A-IFM $[Ca^{2+}]$, bilateral power balancing via the thoracic exoskeleton and potentially strain-dependent power augmentation owing to an increase in stroke amplitude during manoeuvring flight [24].

4. Conclusions

Our study shows that within the locomotor range of tethered flying *D. melanogaster*, $[Ca^{2+}]$ inside the A-IFM linearly increases with increasing power requirements for flight. This result matches previous findings on isolated, skinned A-IFM fibres of the fruit fly using work-loop analysis [24,26] and also calcium estimations, when calcium was correlated with the changes in aerodynamic power and A-IFM motor nerve firing frequency [19]. Despite up to 4000 times the smaller muscle power output of isolated fibres compared with the mechanical power required for wing flapping, our results demonstrate that calcium-dependent control of muscle power is comparable in intact and dissected fibres of the A-IFM [23,24,71,72]. In both cases, power output owing to calcium- and stretch activation varies within a comparatively small

range of intramuscular calcium levels from 56 to 79 nM (mean of all A-IFM fibres, for conversion method see the electronic supplementary material, figure 3*b*).

Matching the production of flight muscle mechanical power to the power requirements needed for wing flapping might yield benefits in flying insects. If the animal provides calcium-depended mechanical power in excess to what is actually needed for wing flapping, the wing hinge must destroy waste power to avoid changes in wing kinematics. Alternatively, the animal might allow power-driven changes in wing kinematics at the potential cost of changes in flight direction and body instabilities. Moreover, a destruction of waste power might lead to a significant degradation of muscle and flight efficiency, which in turn might harm the biological fitness of flying animals. This is of interest because in insects flight muscle efficiency is relatively small, ranging from low 3 per cent in locust [73] to a maximum of 16 per cent in *Euglossine* bees [74], and total flight efficiency in *Drosophila* amounts to a maximum of only 4 per cent [75]. Alternatively, if *Drosophila* may not sufficiently provide instantaneous mechanical power, power transmission to the wings may fail when flight control muscles reconfigure wing hinge mechanics during manoeuvring flight. Calcium-mediated control of power thus helps to precisely match A-IFM mechanical power output to the actual energetic needs for flight.

The bilateral shift of A-IFM power by the thoracic shell thereby might help to broadly provide and balance power between both body sides, whereas the fly finely controls calcium of the A-IFM by gradually changing its motor neuron spike frequency in synchrony with steering [4,19,56]. The bilateral control of $[Ca^{2+}]$ inside the A-IFM runs, moreover, counter to the hypothesis that the thorax of *Drosophila* acts as a single, equally proportional source for mechanical power production for both wings [70]. In conclusion, dissections of the mechanisms for flight power control allow us to refine our understanding of how insects balance power inside the thorax shell and budget their energy expenditure during manoeuvring flight. Eventually, any energetic benefit from power control would be of great interest in the field of biomimetic aircraft design because flapping-winged aircraft are mainly challenged by the high-power requirements of flapping flight [76,77].

We thank Ursula Seifert for comments on the manuscript. This research was supported by grants of the German Science Foundation LE905/10–1 and the Ministry of Education and Research BioFuture 0311885 to F.O.L.

References

1. Dickinson MH, Tu MS. 1997 The function of Dipteran flight muscle. *Comp. Biochem. Physiol. A* **116A**, 223–238. (doi:10.1016/S0300-9629(96)00162-4)
2. Götz KG. 1983 Bewegungssehen und Flugsteuerung bei der Fliege *Drosophila*. In *BIONA-report 2* (ed. W Nachtigall), pp. 21–34. Stuttgart, Germany: Fischer.
3. Heide G. 1983 Neural mechanisms of flight control in *Diptera*. In *BIONA-report 2* (ed. W Nachtigall), pp. 35–52. Stuttgart, Germany: Fischer.
4. Heide G, Spüler M, Götz KG, Kamper K. 1985 Neural control of asynchronous flight muscles in flies during induced flight manoeuvers. In *Insect locomotion* (ed. G Wendler), pp. 215–222. Berlin, Germany: Paul Parey.
5. Pringle JWS. 1978 Stretch activation of muscle: function and mechanism. *Proc. R. Soc. Lond. B* **201**, 107–130. (doi:10.1098/rspb.1978.0035)
6. Tu MS, Dickinson MH. 1996 The control of wing kinematics by two steering muscles of the blowfly, *Calliphora vicina*. *J. Comp. Physiol. A* **178**, 813–830. (doi:10.1007/BF00225830)
7. Dickinson MH, Lighton JRB. 1995 Muscle efficiency and elastic storage in the flight motor of *Drosophila*. *Science* **268**, 87–89. (doi:10.1126/science.7701346)
8. Balint CN, Dickinson MH. 2001 The correlation between wing kinematics and steering muscle activity in the blowfly *Calliphora vicina*. *J. Exp. Biol.* **204**, 4213–4226.
9. Egelhaaf M. 1989 Visual afferences to flight steering muscles controlling optomotor responses of the fly. *J. Comp. Physiol. A* **165**, 719–730. (doi:10.1007/BF00610871)
10. Heide G, Götz KG. 1996 Optomotor control of course and altitude in *Drosophila melanogaster* is correlated with distinct activities of at least three pairs of flight steering muscles. *J. Exp. Biol.* **199**, 1711–1726.
11. Götz KG. 1968 Flight control in *Drosophila* by visual perception of motion. *Biol. Cybern.* **4**, 199–208. (doi:10.1007/BF00272517)
12. Lehmann F-O, Dickinson MH. 1997 The changes in power requirements and muscle efficiency during elevated force production in the fruit fly, *Drosophila melanogaster*. *J. Exp. Biol.* **200**, 1133–1143.
13. Tu MS, Dickinson MH. 1994 Modulation of negative work output from a steering muscle of the blowfly *Calliphora vicina*. *J. Exp. Biol.* **192**, 207–224.
14. Wang H, Ando N, Kanzaki R. 2008 Active control of free flight manoeuvres in a hawkmoth, *Agrius convolvuli*. *J. Exp. Biol.* **211**, 423–432. (doi:10.1242/jeb.011791)
15. Dickinson MH, Lehmann F-O, Sane S. 1999 Wing rotation and the aerodynamic basis of insect flight. *Science* **284**, 1954–1960. (doi:10.1126/science.284.5422.1954)
16. Josephson RK, Young D. 1985 A synchronous insect muscle with an operating frequency greater than 500 Hz. *J. Exp. Biol.* **118**, 185–208.
17. Josephson RK, Malamud JG, Stokes DR. 2000 Asynchronous muscle: a primer. *J. Exp. Biol.* **203**, 2713–2722.
18. Pringle JWS. 1968 Comparative physiology of the flight motor. *Adv. Insect Physiol.* **5**, 163–227. (doi:10.1016/S0065-2806(08)60229-5)
19. Gordon S, Dickinson MH. 2006 Role of calcium in the regulation of mechanical power in insect flight. *Proc. Natl Acad. Sci. USA* **103**, 4311–4315. (doi:10.1073/pnas.0510109103)
20. Josephson RK. 1999 Dissecting muscle power output. *J. Exp. Biol.* **202**, 3369–3375.
21. Rome LC, Lindstedt SL. 1998 The quest for speed: muscles built for high-frequency contractions. *News Physiol. Sci.* **13**, 261–268.
22. Gilmour KM, Ellington CP. 1993 Power output of glycerinated bumblebee flight muscle. *J. Exp. Biol.* **183**, 77–100.
23. Tohtong R, Yamashita H, Graham M, Haeberle J, Simcox A, Maughan D. 1995 Impairment of muscle function caused by mutations of phosphorylation sites in myosin regulatory light chain. *Nature* **374**, 650–653. (doi:10.1038/374650a0)
24. Wang Q, Zhao C, Swank DM. 2011 Calcium and stretch activation modulate power generation in *Drosophila* flight muscle. *Biophys. J.* **101**, 2207–2213. (doi:10.1016/j.bpj.2011.09.034)
25. Granzier HL, Wang K. 1993 Passive tension and stiffness of vertebrate skeletal and insect flight muscles: the contribution of weak cross-bridges and elastic filaments. *Biophys. J.* **65**, 2141–2159. (doi:10.1016/S0006-3495(93)81262-1)
26. Swank DM. 2012 Mechanical anaylsis of *Drosophila* indirect flight and jump muscles. *Methods* **56**, 69–77. (doi:10.1016/j.ymeth.2011.10.015)
27. Josephson RK, Syme DA. 2001 How to build fast muscles. II. Asynchronous muscle: a design breakthrough. *Am. Zool.* **41**, 1488–1489.
28. Moore JR. 2006 Stretch activation: towards a molecular mechanism. In *Nature's versatile engine: insect flight muscle inside and out* (ed. JO Vigoreaux), pp. 44–60. New York, NY: Springer.
29. Peckham M, Cripps R, White D, Bullard B. 1992 Mechanics and protein content of insect flight muscles. *J. Exp. Biol.* **168**, 57–76.
30. Thomas N, Thornhill RA. 1994 Stretch activation of cross-bridges in fibrillar insect flight muscle. *J. Physiol.* **0**, 76P–77P.
31. Thomas N, Thornhill RA. 1995 A theory of tension fluctuations due to muscle cross-bridges.

Proc. R. Soc. Lond. B **259**, 235–242. (doi:10.1098/rspb.1995.0035)

32. Thomas N, Thornhill RA. 1996 Stretch activation and nonlinear elasticity of muscle cross-bridges. *Biophys. J.* **70**, 2807–2818. (doi:10.1016/S0006-3495(96)79850-8)
33. Moore JR, Dickinson MH, Vigoreaux JO, Maughan DW. 2000 The effect of removing the N-terminal extension of the *Drosophila* myosin regulatory light chain upon flight ability and the contractile dynamics of indirect flight muscle. *Biophys. J.* **78**, 1431–1440. (doi:10.1016/S0006-3495(00)76696-3)
34. Ramanath S, Wang Q, Bernstein SI, Swank DM. 2011 Disrupting the myosin converter–relay interface impairs *Drosophila* indirect flight muscle performance. *Biophys. J.* **101**, 1114–1122. (doi:10.1016/j.bpj.2011.07.045)
35. Swank DM, Braddock JM, Brown W, Lesage H, Bernstein SI, Maughan DW. 2006 An alternative domain near the ATP binding pocket of *Drosophila* myosin affects muscle fiber kinetics. *Biophys. J.* **90**, 2427–2435. (doi:10.1529/biophysj.105.075184)
36. Yang C, Ramanath S, Kronert WA, Berstein SI, Maughan DW, Swank DM. 2008 Alternative versions of the myosin relay domain differently respond to load to influence *Drosophila* muscle kinetics. *Biophys. J.* **95**, 5228–5237. (doi:10.1529/biophysj.108.136192)
37. Yang C, Kaplan CN, Thatcher ML, Swank DM. 2010 The influence of myosin converter and relay domains on corss-bridge kinetics of *Drosophila* indirect flight muscle. *Biophys. J.* **99**, 1546–1555. (doi:10.1016/j.bpj.2010.06.047)
38. Katzemich A, Kreisköther N, Alexandrovich A, Elliott C, Schöck F, Leonard K, Sparrow JC, Bullard B. 2012 The function of the M-line protein obscurin in the controlling the symmetry of the sarcomere in the flight muscle of *Drosophila*. *J. Cell Sci.* **125**, 3367–3379. (doi:10.1242/jcs.097345)
39. Kržič U, Vladimir R, Leonard KR, Linke WA, Bullard B. 2010 Regulation of the oscillatory contraction in insect flight muscle by troponin. *J. Mol. Biol.* **397**, 110–118. (doi:10.1016/j.jmb.2010.01.039)
40. Barton B, Ayer G, Heymann N, Maughan DW, Lehmann F-O, Vigoreaux JO. 2005 Flight muscle properties and aerodynamic performance of *Drosophila* expressing a *flightin* gene. *J. Exp. Biol.* **208**, 549–560. (doi:10.1242/jeb.01425)
41. Miller MS, Lekkas P, Braddock JM, Farman GP, Ballif BA, Irving TC, Maughan DW, Vigoreaux JO. 2008 Aging enhances indirect flight muscle performance yet decreases flight ability in *Drosophila*. *Biophys. J.* **95**, 2391–2401. (doi:10.1529/biophysj.108.130005)
42. Eckert H. 1973 Optomotorische Untersuchungen am visuellen System der Stubenfliege *Musca domestica* L. *Kybernetik* **14**, 1–23. (doi:10.1007/BF00290291)
43. Götz KG. 1964 Optomotorische Untersuchung des visuellen Systems einiger Augenmutanten der Fruchtfliege *Drosophila*. *Kybernetik* **2**, 77–92. (doi:10.1007/BF00288561)
44. Casey TM. 1981 A comparison of mechanical and energetic estimates of flight cost for hovering sphinx moths. *J. Exp. Biol.* **91**, 117–129.
45. Dickinson MH, Lehmann F-O, Chan WP. 1998 The control of mechanical power in insect flight. *Am. Zool.* **38**, 718–728. (doi:10.1093/icb/38.4.718)
46. Ellington CP. 1984 The aerodynamics of hovering insect flight. VI. Lift and power requirements. *Phil. Trans. R. Soc. Lond. B* **305**, 145–181. (doi:10.1098/rstb.1984.0054)
47. Ellington CP. 1985 Power and efficiency of insect flight muscle. *J. Exp. Biol.* **115**, 293–304.
48. Demerec M. 1965 *Biology of* Drosophila. New York, NY: Hafner Publishing Company.
49. Lehmann F-O, Dickinson MH. 1998 The control of wing kinematics and flight forces in fruit flies (*Drosophila* spp.). *J. Exp. Biol.* **201**, 385–401.
50. Diegelmann S, Fiala A, Leibold C, Spall T, Buchner E. 2002 Transgenic flies expressing the fluorescence calcium sensor cameleon 2.1 under UAS control. *Genesis* **34**, 95–98. (doi:10.1002/gene.10112)
51. Fan GY, Fujisaki H, Miyawaki A, Tsay R-K, Tsien RY, Ellisman MH. 1999 Video-rate scanning two-photon excitation fluorescence microscopy and ratio imaging with cameleons. *Biophys. J.* **76**, 2412–2420. (doi:10.1016/S0006-3495(99)77396-0)
52. Miyawaki A, Griesbeck O, Heim R, Tsien RY. 1999 Dynamic and quantitative Ca^{2+} measurements using improved cameleons. *Proc. Natl Acad. Sci. USA* **96**, 2135–2140. (doi:10.1073/pnas.96.5.2135)
53. Miyawaki A, Tsien RY. 2000 Monitoring protein conformations and interactions by fluorescence resonance energy transfer between mutants of green fluorescent protein. *Methods Enzymol.* **327**, 472–500. (doi:10.1016/S0076-6879(00)27297-2)
54. Miyawaki A, Llopis J, Heim R, McCaffery JM, Adams JA, Ikura M, Tsien RY. 1997 Fluorescent indicators for Ca^{2+} based on green fluorescent proteins and calmodulin. *Nature* **388**, 882–887. (doi:10.1038/42264)
55. Truong K, Sawano A, Mizuno H, Hama H, Tong KI, Mal TK, Miyawaki A, Mitsuhiko I. 2001 FRET-based *in vivo* Ca^{2+} imaging by a new calmodulin–GFP fusion molecule. *Nat. Struct. Biol.* **8**, 1069–1073.
56. Harcombe ES, Wyman RJ. 1978 The cyclically repetitive firing sequences of identified *Drosophila* flight motorneurons. *J. Comp. Physiol. A* **123**, 271–279. (doi:10.1007/BF00656881)
57. Trimarchi JR, Schneiderman AM. 1994 The motor neurons innervating the direct flight muscles of *Drosophila melanogaster* are morphologically specialized. *J. Comp. Neurol.* **340**, 427–443. (doi:10.1002/cne.903400311)
58. Borst A. 1990 How do flies land? *BioScience* **40**, 292–299. (doi:10.2307/1311266)
59. Chan WP, Dickinson MH. 1996 *In vivo* length oscillations of indirect flight muscles in the fruit fly *Drosophila virilis*. *J. Exp. Biol.* **199**, 2767–2774.
60. Agianian B, Krzic U, Qiu F, Linke WA, Leonard K, Bullard B. 2004 A troponin switch that regulates muscle contraction by stretch instead of calcium. *EMBO* **23**, 772–779. (doi:10.1038/sj.emboj.7600097)
61. Iwamoto H, Inoue K, Yagi N. 2010 Fast x-ray recordings reveal dynamic action of contractile and regulatory proteins in stretch-activated insect flight muscle. *Biophys. J.* **99**, 184–192. (doi:10.1016/j.bpj.2010.04.009)
62. Linari M, Reedy MK, Reedy MC, Lombardi V, Piazzesi G. 2004 Ca-activation and stretch activation in insect flight muscle. *Biophys. J.* **87**, 1101–1111. (doi:10.1529/biophysj.103.037374)
63. Rome LC. 1990 Influence of temperature on muscle recruitment and muscle function *in vivo*. *Am. J. Physiol.* **259**, R210–R222.
64. Dudley R. 2000 The evolutionary physiology of animal flight: paleobiological and present perspectives. *Ann. Rev. Physiol.* **62**, 135–155. (doi:10.1146/annurev.physiol.62.1.135)
65. Miller PL. 1966 The supply of oxygen to the active flight muscles of some large beetles. *J. Exp. Biol.* **45**, 285–304.
66. Wigglesworth VB, Lee WM. 1982 The supply of oxygen to the flight muscles of insects: a theory of tracheole physiology. *Tiss. Cell* **14**, 501–518. (doi:10.1016/0040-8166(82) 90043-X)
67. Lehmann F-O, Sane SP, Dickinson MH. 2005 The aerodynamic effects of wing–wing interaction in flapping insect wings. *J. Exp. Biol.* **208**, 2075–3092. (doi:10.1242/jeb.01744)
68. Shishkin A, Schützner P, Wagner C, Lehmann F-O. 2012 Experimental quantification and numerical simulation of unsteady flow conditions during free flight maneuvers in insects. In *Nature-inspired fluid mechanics* (eds C Tropea, H Bleckmann), pp. 81–99. Berlin, Germany: Springer.
69. Mronz M, Lehmann F-O. 2008 The free flight response of *Drosophila* to motion of the visual environment. *J. Exp. Biol.* **211**, 2026–2045. (doi:10.1242/jeb.008268)
70. Götz KG, Wandel U. 1984 Optomotor control of the force of flight in *Drosophila* and *Musca* II. Covariance of lift and thrust in still air. *Biol. Cybern.* **51**, 135–139. (doi:10.1007/BF00357927)
71. Dickinson MH *et al*. 1997 Phosphorylation-dependent power output of transgenic flies: an integrated study. *Biophys. J.* **7**, 3122–3134. (doi:10.1016/S0006-3495(97)78338-3)
72. Liu H, MIller MS, Swank DM, Kronert WA, Maughan DW. 2005 Paramyosin phosphorylation site disruption affects indirect flight muscle stiffness and power generation in *Drosophila melanogaster*. *Proc. Natl Acad. Sci. USA* **102**, 10 522–10 527. (doi:10.1073/pnas.0500945102)
73. Josephson RK, Stevenson RD. 1991 The efficiency of a flight muscle from the locust, *Schistocera americana*. *J. Physiol.* **442**, 413–429.
74. Casey TM, Ellington CP. 1989 Energetics of insect flight. In *Energy transformations in cells and organisms* (eds W Wieser, E Gnaiger), pp. 200–210. Stuttgart, Germany: Thieme.
75. Lehmann F-O. 2001 The efficiency of aerodynamic force production in *Drosophila*. *J. Comp. Physiol. A* **131**, 77–88. (doi:10.1016/S1095-6433(01) 00467-6)
76. Ellington CP. 1999 The novel aerodynamics of insect flight: applications to micro-air vehicles. *J. Exp. Biol.* **202**, 3439–3448.
77. Stafford N. 2007 Spy in the sky. *Nature* **445**, 808–809. (doi:10.1038/445808a)